NASA TECHNICAL MEMORANDUM

NASA TM X-3353

NASA TM X-3353

SYSTEM TESTS WITH ELECTRIC THRUSTER BEAM AND ACCELERATOR DIRECTLY POWERED FROM LABORATORY SOLAR ARRAYS

John B. Stover

Lewis Research Center

Cleveland, Ohio 44135

NATIONAL AERONAUTICS AND SPACE ADMINISTRATION • WASHINGTON, D. C. • APRIL 1976

1. Report No.	2. Government Accession No.	3. Recipient's Catalog No.
NASA TM X-3353		

4. Title and Subtitle	5. Report Date
SYSTEM TESTS WITH ELECTRIC THRUSTER BEAM AND ACCELERATOR DIRECTLY POWERED FROM LABORATORY SOLAR ARRAYS	April 1976
	6. Performing Organization Code
7. Author(s)	8. Performing Organization Report No.
John B. Stover	E-8546
	10. Work Unit No.
9. Performing Organization Name and Address	506-23
Lewis Research Center National Aeronautics and Space Administration Cleveland, Ohio 44135	11. Contract or Grant No.
	13. Type of Report and Period Covered
12. Sponsoring Agency Name and Address	Technical Memorandum
National Aeronautics and Space Administration Washington, D. C. 20546	14. Sponsoring Agency Code

15. *Supplementary Notes*

16. Abstract

Laboratory high voltage solar arrays were operated directly connected to power the beam and accelerator loads of an 8-centimeter ion thruster. The beam array comprised conventional 2 by 2 centimeter solar cells; the accelerator array comprised multiple junction edge-illuminated solar cells. Conventional laboratory power supplies powered the thruster's other loads. Tests were made to evaluate thruster performance and to investigate possible electrical interactions between the solar arrays and the thruster. Thruster performance was the same as with conventional laboratory beam and accelerator power supplies. Most of the thruster beam short circuits that occurred during solar array operation were cleared spontaneously without automatic or manual intervention. No spontaneous clearing occurred during conventional power supply operation.

17. Key Words (Suggested by Author(s))	18. Distribution Statement
Solar cells Electric propulsion Thruster Propulsion system High voltage	Unclassified - unlimited STAR Category 20

19. Security Classif. (of this report)	20. Security Classif. (of this page)	21. No. of Pages	22. Price*
Unclassified	Unclassified	27	$3.75

* For sale by the National Technical Information Service, Springfield, Virginia 22161

SYSTEM TESTS WITH ELECTRIC THRUSTER BEAM AND ACCELERATOR DIRECTLY POWERED FROM LABORATORY SOLAR ARRAYS

by John B. Stover

Lewis Research Center

SUMMARY

Electrical system tests were made with laboratory high voltage solar arrays directly connected to power the beam and accelerator loads of an 8-centimeter ion thruster. The beam array comprised conventional 2 by 2 centimeter solar cells; the accelerator array comprised multiple junction edge-illuminated solar cells. The thruster's ionizing discharge and other loads were operated from a standard set of laboratory thruster power supplies. The purpose of the tests was to evaluate the solar array - thruster performance and to investigate possible electrical interactions between the solar arrays and their thruster loads. Test results are applicable to the design of a space flight electrical system for an ion thruster powered by a high voltage solar array.

Thruster performance data and steady-state and transient waveforms were recorded during operation of the thruster from the solar arrays. Comparison data for thruster operation from conventional high voltage laboratory power supplies were also recorded. Steady-state performance and waveforms were essentially the same regardless of whether the beam and accelerator loads were directly powered from solar arrays or from conventional power supplies.

The thruster operated quietly from either the solar arrays or conventional power supplies with only infrequent beam short circuits. Most of the beam short circuits that occurred during solar array operation were cleared spontaneously without automatic or manual intervention. (No spontaneous clearing occurred during conventional power supply operation.) Of those short circuits not cleared spontaneously, most were cleared by momentary reduction of discharge emission current.

Oscillograms were made of transient voltage excursions during the spontaneous clearing of beam short circuits. A simple electrical model of the solar arrays is adequate to represent array transient performance. The model comprises the usual constant current generator and diode combination with a lumped capacitor added to represent the solar array distributed capacitance to the facility ground (laboratory solar array heat sink potential). The physical electronic mechanism by which spontaneous clearing was initiated is not clear.

INTRODUCTION

The results are presented herein of system tests with laboratory high voltage solar arrays directly connected to power both the beam and accelerator loads of an 8-centimeter ion thruster.

A regulated high voltage solar array (HVSA) has definite advantages for supplying some spacecraft loads. To provide solar electric power to such high voltage spacecraft loads as traveling wave tubes and ion thrusters, an electronic power processor is used to convert dc power from a low voltage solar cell array (output voltage of perhaps 60 V) to dc power (output voltage of 1000 to 16 000 V). The power processor will in some cases weigh more than the load, have a degree of inefficiency with a corresponding amount of heat rejection to the spacecraft, and include hundreds of electronic components that must all work together reliably. When high voltage loads are comparatively large and use a major fraction of the total solar array electric power output, it is important to consider the substitution of a regulated high voltage solar array for that part of the conventional low voltage solar array and its associated power processor.

The concept of a regulated HVSA has been described in references 1 and 2. It features subdividing a solar cell array into blocks, configuring the blocks into interconnected series and/or parallel combinations, and fine controlling the output voltage or current by shunt switching internal to given blocks. The advantages of an HVSA are reduced system weight, increased system electrical efficiency, reduced heat rejection to the spacecraft, increased reliability, elimination of voltage/current ripple generated by the power processor, and inherent fine control of output voltage (ref. 3).

An HVSA technology development program is currently under way at Lewis Research Center. References 4 to 6 report the results of contract studies related to this program. Reference 7 describes a 9-module, 1-kilowatt, laboratory solar cell array (voltage capability up to 15 kV) that was built under contract and installed at Lewis in support of this development program. A tenth engineering development module, built under the same contract, was used for the tests reported herein.

The purpose of the electric thruster system tests reported herein was to determine the performance of a system in which certain elements of an ion thruster were operated directly from dedicated high voltage solar arrays and to investigate any possible electrical interactions between the solar arrays and their thruster loads. One solar array consisted of conventional 2 by 2 centimeter solar cells electrically configured to directly power the thruster beam. The other array consisted of multiple-junction edge-illuminated cells electrically configured to power the thruster accelerator. Of major interest was the effect of the solar arrays on thruster steady-state electrical parameters and waveforms and the system response to thruster beam short circuits.

APPARATUS

An ion thruster, a console of thruster power supplies, and two laboratory high voltage solar arrays were used for the system tests. Interface electrical circuits joined these elements.

Thruster

References 8 and 9 describe an 8-centimeter electron bombardment mercury ion thruster of the type used. The thruster was mounted to exhaust downward within an 80-centimeter (32-in.) diameter, 150-centimeter (5-ft) high vacuum tank. The pressure was typically 2666 micropascals (2×10^{-5} torr) during thruster operation. The thruster beam impinged on a carbon emulsion coated stainless-steel target designed to reduce backsputtering.

The thruster is a complex electrical load that includes three interacting plasma discharges. Mutually, these discharges determine the characteristics of the beam and accelerator loads. Figure 1 illustrates schematically the thruster's major parts interconnected with the several required power supplies. Correct operation of the thruster's beam and accelerator loads, at rated current and voltage, depends on the mutual adjustment and control of all of the required power supplies.

Thruster Power Supplies

Reference 9 describes a standard console of laboratory thruster power supplies of the type used in these tests. The console includes the 4 ac (60 Hz) and 5 dc (60 Hz full wave rectified) adjustable voltage power supplies and a voltage-limiting network (fig. 1). It also includes the several electrical meters (3 percent accuracy, panel type) and thermocouple meters required to measure the thruster operating parameters. In the particular console used, the mercury propellant flow rate was manually controlled rather than automatically controlled as indicated in reference 9.

In figure 1 the power supplies labeled V_{CV} (cathode vaporizer), V_{CH} (cathode heater), V_{CK} (cathode keeper), and ΔV_I (main discharge) are associated with the production of the mercury propellant ionizing discharge within the thruster. Those supplies labeled V_I (beam) and V_A (accelerator) are associated with extraction and acceleration of ions from the thruster. The supplies labeled V_{NV} (neutralizer vaporizer), V_{NH} (neutralizer heater), and V_{NK} (neutralizer keeper) are associated with producing a source of electrons to neutralize the ion exhaust beam.

Laboratory Solar Arrays

Reference 7 describes the HVSA and the HVSA support module used to power the thruster's ion beam load; a smaller array to power the thruster's accelerator load was also installed in the same support module. Figure 2(a) illustrates the 2560 series-connected 2 by 2 centimeter 10 ohm-centimeter silicon solar cells which supply 72 milliamperes to the thruster's 1220-volt ion beam load. Groups of 16, 32, 64, and 128 cells are shunted by shorting switches for the purpose of adjusting array voltage to within 1 percent of rated beam voltage. Figure 2(b) illustrates 20 series-connected 96-junction edge-illuminated solar cells (ref. 10) clamped by Zener diodes to supply 500 volts for the accelerator at currents between 0 and 0.4 milliampere.

The HVSA support module, which provides illumination and cooling for these two solar arrays, is shown in the right foreground of figure 3. The two sides of the module hinge downward for access to the solar cells mounted on one side and to the lamps mounted on the second side. A dc power supply provides power to twenty 500-watt tungsten iodide lamps to illuminate the solar cells. Ducted air flow cools both the lamps and an infrared filter which separates the lamps and the array. The set of four manually operated cell-shorting switches shown in figure 2(a) is mounted in a switch box at one end of the HVSA support module.

In figure 4 the solar arrays are shown mounted on the inner face of one support module side which has been hinged downward to a horizontal position. The array of 2560 2 by 2 centimeter cells, cemented to a 0.126-millimeter- (5-mil-) thick Kapton (polyimide film) substrate, occupies most of the area visible in the figure. A small 0.711-millimeter (28-mil) G-10 fiberglass circuit board, which mounts 20 multiple junction edge-illuminated solar cells, is visible at the right. The circuit board, cells, and Zener diodes are also cemented to the Kapton substrate. Bypass diodes for the larger array can also be seen at its right and left ends. The substrate is attached to a frame closely fitted over a water-cooled heat sink built into the hinged side of the support module. (A layer of 0.711-mm (28-mil) G-10 fiberglass electrical insulation is cemented to the face of the heat sink.) A partial vacuum is maintained between the substrate and the heat sink to assure adequate contact pressure for heat conduction.

Interface Circuits

Figure 5 shows a schematic diagram of the interconnection circuits between the solar cell arrays, laboratory thruster power supplies, and ion thruster. These circuits permit quick change of thruster beam and accelerator loads from conventional electronic power supply to solar array operation. They also permit quick change between two alternate points of beam supply connection to the thruster. During solar array - thruster

operation it is possible to momentarily short or disconnect either array, or both. Short-circuit, open-circuit, and load voltages and currents of both solar arrays may conveniently be verified during each data run. Electrical meters are of the same type and accuracy as those in the thruster laboratory power supply consoles.

EXPERIMENTAL PROCEDURE

Two types of tests were made. Steady-state performance data were obtained for conventional high voltage power supply- and HVSA-thruster operation. For HVSA-thruster operation, transient voltage excursions were recorded during spontaneous clearing of beam short circuits.

Thruster Operation

With the thruster tank vacuum at 13.33 micropascals (1×10^{-7} torr), the thruster's neutralizer and main discharge were started from the standard console of thruster power supplies. The beam and accelerator loads were powered alternately from the high voltage solar arrays and from the console's high voltage power supplies. Thruster operation was controlled by the manual adjustment of the console power supplies to the standard set of electrical parameters shown in table I. Approximately 2 hours of operation were required to attain thermal equilibrium between the thruster and its vacuum tank.

Correct thruster operation is largely dependent on the simultaneous control of main vaporizer heater current, main discharge voltage, and discharge emission current to produce rated beam current at rated beam voltage. In some thruster power supply consoles this simultaneous control is automatic; in the console used for these tests the control is manual. The result of manual control in the tests was drift of thruster parameters to a degree which was tolerable only after a few hours of operation and approximately a dozen control iterations.

Solar Array Operation

The solar array support module was started, prior to thruster operation, by turning on (1) the array heat sink cooling water to about 175 cubic centimeters per second (2.75 g/min), (2) the lamp cooling fans, and (3) the auxiliary vacuum to about 77 000 pascals (7 in. Hg, gage). The beam array shorting switch was closed and lamp voltage was increased until beam solar array short-circuit current was 120 milliamperes. Corresponding short-circuit current for the accelerator array was 1.4 milliamperes. (In

some tests, for the purpose of operating the thruster closer to the beam array's maximum power point, illumination was reduced so that beam array short-circuit current was about 90 mA.) Open-circuit voltage, short-circuit current, and load voltages and currents were recorded before, during, and after experimental runs. Beam voltage at rated beam current was adjusted by means of shorting switches across the appropriate cell groups.

Performance Comparison Tests

Steady-state thruster operation was established at the electrical parameter set shown in table I. Thruster electrical parameters were recorded from the calibrated panel meters of the interface console and the thruster power supply console. Propellant flow rates were measured by timing the flow of known volumes of mercury to the thruster through a standard burette feed system. Interchanges between conventional electronic beam and accelerator power supplies and the solar arrays were accomplished quickly by means of the interface switches. Rapid switching ensured valid comparisons under comparable thruster operating conditions, regardless of any residual drift of parameters during manually controlled steady-state thruster operation. Oscillograms were obtained of steady-state waveforms of beam and accelerator voltages, beam and emission currents, and neutralizer coupling voltage. Comparison waveforms, between conventional power supply and solar array thruster operation, were obtained within a period of 1 to 2 minutes.

HVSA-Thruster Transient Tests

Spontaneous clearing of beam short circuits, during steady-state operation of the thruster on solar arrays, was observed and recorded during the performance comparison tests. A thruster beam short circuit occurs when accelerator voltage is momentarily decreased toward zero and below a threshold level. Then, electron backstreaming from the neutralizer into the main discharge chamber overloads the beam power supply and results in a reduction of beam voltage. This voltage reduction results in increased accelerator ion impingement current, which overloads the accelerator power supply. Accelerator voltage may remain low long enough to cause the beam short circuit to persist.

For the purposes of the tests reported here, a beam short circuit was forced to occur by momentarily closing the accelerator solar array shorting switch. Although the beam short circuit was forced, the voltage excursions that occurred afterward were spontaneous. Voltage excursions of both solar arrays, which occurred simultaneously

one to several seconds after opening the shorting switch, were recorded on a storage type oscilloscope. Traces of each voltage were recorded in turn. Their time correlation was established both by accurate adjustment of oscilloscope triggering level and by applying one voltage to the vertical input and one to the horizontal input to obtain their crossplot on the oscilloscope screen during spontaneous clearing of a beam short circuit.

RESULTS AND DISCUSSION

Steady-state performance comparison and HVSA-thruster transient tests were made. Steady-state data sets and selected electrical waveforms were recorded alternately during thruster operation from conventional high voltage power supplies and from HVSAs. Transient excursions of HVSA-thruster beam and accelerator voltages were recorded during spontaneous clearing of beam short circuits.

Steady-State Performance Comparison Tests

Because a laboratory thruster, rather than a flight-type thruster, was used in the tests, it was anticipated that best operation might possibly occur at other than nominal parameters. Also, quiet, steady waveforms are preferred to noisy, choppy ones simply because solar arrays have little inherent capacitance to supply bursts of electrical charge. For both of these reasons the nominal set of thruster operating parameters was experimentally revised. A tabulation of parameters used as standard in the system tests is shown in table I; also shown is a tabulation of corresponding parameters from reference 8. A notable difference is that accelerator drain current was almost three times as high in the present tests as in reference 8. Emission current was somewhat lower, and propellant flow was somewhat higher than for the reference thruster. The neutralizer coupling voltage turned out to be over twice as large for the thruster used in these tests. Contrary to the reference case, some cathode heater current was required during operation at the 4.45-millinewton (1-mlb) thrust level; also, cathode keeper current was higher. The upshot of these differences is somewhat lower, but not unrepresentative, power efficiency, propellant utilization, and specific impulse for the thruster used in these system tests. These figures also appear in table I.

As is apparent from a comparison of columns one and two of table I, the overall operation was the same whether conventional power supplies (column 1) or solar arrays (column 2) powered the thruster beam and accelerator loads. Also, alternative connections of the beam supply to the thruster anode or cathode made no difference. (The beam supply voltage was, of course, reduced by an amount equal to the discharge voltage when connected to the thruster cathode.)

To identify and to understand any differences in thruster operation between conventional power supply and solar array operation, steady-state waveforms were compared. The comparison was between pairs of oscillograms made usually within a 1- to 2-minute period by switching between conventional and solar array supplies. Little significant difference was found between comparison waveforms. Some high frequency components of conventional power supply beam voltage and current waveforms were absent from the corresponding HVSA waveforms. Also, of course, the 120-hertz ripple present in the conventional power supply accelerator voltage waveform was absent from the HVSA waveform.

The four oscillograms shown in figure 6 were made during steady-state operation of the thruster on conventional beam and accelerator power supplies. All four top traces show the sum of ac components of beam voltage V_I and neutralizer coupling voltage V_G. The coupling voltage alone is shown on the bottom trace of figure 6(b) where a 120-hertz component is apparent. This component probably results from the ripple of full-wave-rectified 60-hertz power supplies used to power the thruster's neutralizer. The bottom trace of figure 6(c), which shows beam current, and the bottom trace of figure 6(a), which shows main discharge current, also show the 120-hertz component. This component probably exists because of ripple in the full-wave-rectified 60-hertz power supply used to power the main discharge. The bottom trace of figure 6(d) is the sum of the ac components of the accelerator voltage V_A and the neutralizer coupling voltage V_G; it, too, has a 120-hertz component.

The four oscillograms shown in figure 7 were made during steady-state operation of the thruster on HVSA beam and accelerator supplies. All four top traces show the sum of beam voltage V_I and neutralizer coupling voltage V_G. These traces are comparable to the top traces of figure 6. Although the top traces shown in figure 7 normally have about the same amplitude as those shown in figure 6 (somewhat higher in fig. 7 in this particular case), they lack the high frequency components evident in figure 6. It is believed that these high frequency components originate in the coupling voltage and have been attenuated (in fig. 7 traces) by the filtering effect of the distributed capacitance of the solar cell array to facility ground. The neutralizer coupling voltage V_G (shown in the bottom trace of fig. 7(b) oscillogram) is virtually the same as the corresponding trace in figure 6(b). The elimination of some high frequency components by the solar array is also the only difference evident in the comparison of beam current traces.

In figure 8 are steady-state waveforms corresponding to thruster operation at the standard set of electrical operating parameters but with the beam HVSA short-circuit current reduced from 120 to 90 milliamperes. The major difference between this set of oscillograms and the corresponding ones in figure 7 is the larger amplitude of the ac component of beam voltage (in fig. 8) with the array loaded closer to its maximum power point. This results from the larger dynamic impedance of the solar array near its maximum power point. Beam solar array voltage-current characteristic curves for

short-circuit currents of 120 and 90 milliamperes are shown in figure 9.

Figure 10 shows the variation of a significant control parameter set $\{J_B, \Delta V_I, J_E, \dot{m}_{OC}\}$ during the period when the oscillograms of figures 6 and 7 were made. It illustrates the steady-state residual drift due to manual control of the propellant flow rate $\dot{m}_{OC}$ and the discharge voltage ΔV_I to maintain the emission current J_E and beam current J_B constant at selected values. The drift of the parameters shown in figure 10 is larger than it would be with automatic controls.

HVSA-Thruster Transient Tests

The response of a conventional power processor to a beam short circuit would be to momentarily disconnect the beam and accelerator supplies from the thruster, reduce the main discharge current, reapply the beam and accelerator voltages to the thruster, and restore the main discharge current to its original level. Other adjustments, in anticipation of the possibility of a number of successive beam short circuits, might be to reduce the main propellant flow rate and to adjust various thruster currents and voltages to maintain thruster operating temperatures despite the main discharge current reduction. Such responses are discussed in references 11 and 12, but no such response capability was incorporated in the conventional power supplies used in these system tests.

During the system tests reported herein, beam short circuits were infrequent under standard operating conditions with either conventional or solar array beams and accelerator power supplies. A preliminary attempt was made to document the frequency of beam short circuits by monitoring beam voltage on a strip-chart recorder; a low beam voltage indicated over current and therefore a beam short circuit. Although the frequency of short circuits was not documented, it appeared that HVSA-thruster operation was perhaps less susceptible to beam short circuits than conventional power supply thruster operation. During solar array - thruster system operation, most of the beam short circuits that occurred were cleared spontaneously. (No such spontaneous clearing occurred with conventional power supplies.)

Figure 11(a) illustrates the occurrence of a spark (slight dip at the left) and a beam short circuit followed by a spontaneous recovery (at the right). Figure 11(b) shows the spontaneous recovery trace on a larger scale. Typically, the thruster was short circuited for a period of 1 to 300 seconds (11 sec in fig. 11(b)) and then sponteneously returned to normal operation without any automatic or manual intervention. During a beam short circuit the accelerator voltage was zero and the average beam voltage was 300 volts. The beam voltage was unstable, oscillating between 200 and 400 volts; the fundamental frequency of the oscillation was about 120 hertz.

When beam short circuits did not spontaneously clear, it was almost always possible

to clear them by a momentary manual reduction of discharge emission current to about 50 percent of its operating level. A few beam shorts did occur that could be cleared only by disconnecting them from the beam and accelerator arrays; these did not occur frequently enough to be investigated, but they may have occurred during periods of unusually large propellant flow. Another method used to clear beam short circuits was to manually open and close the interface switches simultaneously. This procedure disconnected both beam and accelerator arrays and reconnected them (without reducing emission current) within a period of approximately 3 seconds. This procedure often failed, possibly because the timing was not correct.

Beam short circuits were forced to occur (during HVSA-thruster operation) by momentarily disconnecting the accelerator solar array from the thruster. Although the beam short was forced, the beam and accelerator voltage excursions that occurred (1 to 300 sec afterward) during spontaneous clearing were in fact spontaneous (sometimes these excursions did not occur at all). Time excursions of beam and accelerator voltage during spontaneous clearing are shown in figure 12. The oscillograms were synchronized (as drawn in fig. 12) by means of an accurate triggering adjustment and by obtaining oscillograms of their simultaneous variation on the oscilloscope horizontal and vertical axes.

The simultaneous variation of beam and accelerator voltage during spontaneous recovery is shown in figure 13(a). Several points are labeled (by reference to fig. 12) with the time at which they occurred during the excursion. Figure 13(b) shows the voltage-current characteristic of both solar arrays; the corresponding time of occurrence labeled points from figure 13(a) are also indicated in figure 13(b). The spontaneous recovery occurred beginning at time zero, corresponding to the zero accelerator array voltage and 1.4-milliampere accelerator array current. At the same instant, the beam array voltage was 400 volts and the beam array current was about 116 milliamperes. As the spontaneous recovery proceded, the conditions of solar array operation progressed along the curves of figure 13(b) passing through like-labeled points on the two curves simultaneously. Ultimately the arrays were operating at points corresponding to normal thruster beam and accelerator voltages and currents.

Figure 14 consists of two curves plotted on the same set of axes. The ordinate is current (from 0 to 120 mA) and represents both thruster beam current and beam solar array current. The abscissa is current (from 0 to 1.4 mA) and represents both thruster accelerator current and accelerator solar array current. The dashed curve shows simultaneous values of thruster beam and accelerator currents during the joint variation of beam and accelerator voltages shown in figure 13(a). Again, corresponding time labels are tagged to points on the curve. These current pairs were obtained in an auxiliary test by operating the thruster on the conventional laboratory power supplies; voltages were adjusted to paired values corresponding to points on the excursion, and thruster currents were measured. The solid line curve is merely a plot of the pairs

of solar array currents corresponding to the time-labeled points marked on the array characteristic curves (fig. 13(b)).

If it is assumed that during spontaneous clearing voltage excursions the solar arrays delivered the currents that would be expected from their static voltage-current characteristics, some calculations can be made. Figure 14 shows an 18 milliampere excess in beam array current and a 0.8 milliampere excess in accelerator array current at 0.6 millisecond. The slopes of the curves in figure 12, at 0.6 millisecond, indicate the beam voltage was rising at 1000 volts per millisecond and the accelerator voltage was rising at 330 volts per millisecond. From the previous data and the capacitance charging equation ($i = C(dv/dt)$), effective capacitances of 0.018 and 0.0024 microfarad are estimated for the beam and accelerator arrays, respectively. Estimated effective capacitances based on physical dimensions and material properties are 0.032 and 0.0016 microfarad for beam and accelerator arrays, respectively. Figure 15 shows the solar array equivalent circuit model upon which the foregoing calculation is based. It is suggested that this equivalent circuit model approximately represents transient behavior of the solar arrays during spontaneous recovery from beam short circuits.

Referring again to figure 14, it can be seen that for every pair of time-labeled points on the two curves there is an excess of solar array current over thruster current - except for the time zero point. This excess current means that both arrays, after time zero, can charge their distributed capacitances and cause their terminal voltages to increase toward normal steady-state operating levels. At time zero the accelerator array does not have excess current; it is therefore not clear how the spontaneous recovery begins.

CONCLUDING REMARKS

The HVSA-thruster system test included steady-state and transient waveform and performance data observations of the operation of an 8-centimeter ion thruster's beam and accelerator loads directly from laboratory high voltage solar arrays. Other thruster loads were powered by a standard set of laboratory thruster power supplies. The test was made to investigate electrical interactions, and results are applicable to the design of a spaceflight HVSA-thruster system.

The thruster was manually controlled to a generally stable set of electrical and performance parameters reasonably like published parameter sets. Overall performance was the same, whether beam and accelerator loads were powered by conventional electronic power supplies or by the laboratory solar arrays. Most tests were made with the beam solar array short-circuit current about 1.67 times the normal beam current. Some tests were made with the short-circuit current reduced to 1.25 times the normal beam current to investigate the operation near the solar array's maximum power point.

Steady-state voltage and current waveforms were essentially the same whether beam and accelerator loads were powered by the solar arrays or by conventional laboratory power supplies. Minor differences appeared to be due to a filtering effect of the solar array distributed capacitance. An expected result was that reduced solar array illumination, which caused a beam array short-circuit current reduction of 25 percent, produced increased noise on the beam voltage waveform.

Generally, the thruster ran quietly on either the solar arrays or conventional power supplies with infrequent beam short circuits (coupling of neutralizer and thruster body by backstreaming electrons with the accelerator voltage depressed to near zero). Most of the beam short circuits that occurred during HVSA-thruster operation were spontaneously cleared in a few seconds without automatic or manual intervention. (No such spontaneous clearing occurred during operation with conventional power supplies.) Of the short circuits that were not spontaneously cleared when operating on the HVSA's, most could be cleared by a manual reduction of the main discharge voltage to reduce the emission current to about 50 percent of its operating level.

A constant current generator-diode circuit model of the solar array, with a lumped capacitance added to represent array distributed capacitance, was adequate to represent solar array - thruster transient performance during spontaneous recovery from beam short circuits. For the most part, these transient excursions were quantitatively consistent with this circuit model when used in conjunction with experimentally determined thruster currents at off-normal accelerating voltage combinations.

During spaceflight operation of a solar array - thruster system, thruster beam short circuits could be cleared by a momentary automatic reduction of main discharge emission current. It seems probable that this can be accomplished by a simple modification of the constant-emission-current control presently used in flight-type power processors for the 8-centimeter thruster. It would also be feasible with a simple low-voltage transistor shunt circuit for the case where the discharge is powered by a solar array. Although it is not necessary to routinely clear short circuits by means of inline high voltage switches, it probably will be necessary to have them available on a spaceflight system for backup protection.

Lewis Research Center,
National Aeronautics and Space Administration,
Cleveland, Ohio, December 8, 1975,
506-23.

REFERENCES

1. Herron, B. G.; Bayless, J. R.; and Worden, J. D.: High Voltage Solar Array Technology. AIAA Paper 72-443, Apr. 1972.

2. Triner, James E.: A Digital Regulated Solar Array Power Module. NASA TM X-2314, 1971.

3. Sater, B. L.: The Advantages of the High Voltage Solar Array for Electric Propulsion. AIAA Paper 73-1103, Oct.-Nov. 1973.

4. Springgate, W. F.: High Voltage Solar Array Electrical Configuration Study. (D180-10037-1, Boeing Co.; NAS3-8995) NASA CR-72723, 1970.

5. Herron, B. G.; et al.: High Voltage Solar Array Configuration Study. (Hughes Aircraft Co.; NAS3-8996) NASA CR-72724, 1970.

6. Ebersole, T.; et al.: Study of High Voltage Solar Array Configurations with Integrated Power Control Electronics. (General Electric Co.; NAS3-8997) NASA CR-72725, 1970.

7. Levy, E., Jr.; and Opjorden, R. W.: High Voltage Solar Cell Power Generating System. Tenth Photovoltaic Specialist Conference, Inst. Electrical and Electronics Engrs., Inc., 1974, pp. 123-131.

8. Hudson, W. R.; and Banks, B. A.: An 8-cm Electron Bombardment Thruster for Auxiliary Propulsion. AIAA Paper 73-1131, Oct.-Nov. 1973.

9. 8-cm Mercury Ion Thruster System Technology. Tenth Propulsion Conference, Am. Inst. Aeronautics & Astronautics and Soc. Automotive Engrs., 1974.

10. Sater, B. L.; et al.: The Multiple Junction Edge Illuminated Solar Cell. Tenth Photovoltaic Specialist Conference, Inst. Electrical and Electronics Engrs., Inc., 1974, pp. 188-193.

11. Terdan, F.; and Bechtel, R. T.: Control of a 30-cm-Diameter Mercury Bombardment Thruster. AIAA Paper 73-1079, Oct.-Nov. 1973.

12. Bagwell, James W.; et al.: Review of SERT 2 Power Conditioning. NASA TM X-2085, 1971.

TABLE I. - COMPARISON OF 8-CENTIMETER THRUSTER PERFORMANCE PARAMETERS BETWEEN LABORATORY POWER SUPPLIES AND HIGH VOLTAGE SOLAR ARRAY OPERATION

Description	Laboratory power supplies	Solar cell array	Reference 8 data
Beam current, J_B, mA	72	72	72
Net accelerating voltage, V_I, V	1220	1220	1220
Neutralizer floating potential, V_G, V	-20.1	-19.8	-8
Accelerator voltage, V_A, V	-500	-500	-500
Accelerator drain current, J_A, mA	0.38	0.38	0.135
Discharge voltage, ΔV_I, V	38.0	38.0	40
Emission current, J_E, A	0.77	0.77	1.02
Cathode heater current, J_{CH}, A	2.0	2.0	0
Cathode keeper voltage, V_{CK}, V	13.2	13.2	15.0
Cathode keeper current, J_{CK}, A	0.52	0.52	0.20
Cathode vaporizer temperature, t_{CV}, ^{o}C	270	269	----
Cathode vaporizer flow rate, $\dot{m}_{OC}$, mA	100	100	93
Neutralizer heater current, J_{NH}, A	3.0	3.0	1.5
Neutralizer keeper voltage, V_{NK}, V	17.8	17.8	18.6
Neutralizer keeper current, J_{NK}, A	0.45	0.45	0.50
Neutralizer vaporizer temperature, t_{NV}, ^{o}C	277	278	----
Neutralizer vaporizer flow rate, $\dot{m}_{ON}$, mA	9.6	9.6	6.0
Specific impulse, I_{SP}, sec	2270	2270	2530
Power efficiency, η_P, percent	50.8	50.8	56.4
Total utilization, η_U, percent	65.7	65.7	72.7
Thrust (ideal), T, mN (mlb)	5.07 (1.14)	5.07 (1.14)	5.07 (1.14)
Total neutral flow rate, $\dot{m}_{OTOT}$, mA	109.6	109.6	99.0
Electron volts per ion (including keeper), $\mathscr{E}_{i,k}$, eV	500	500	608

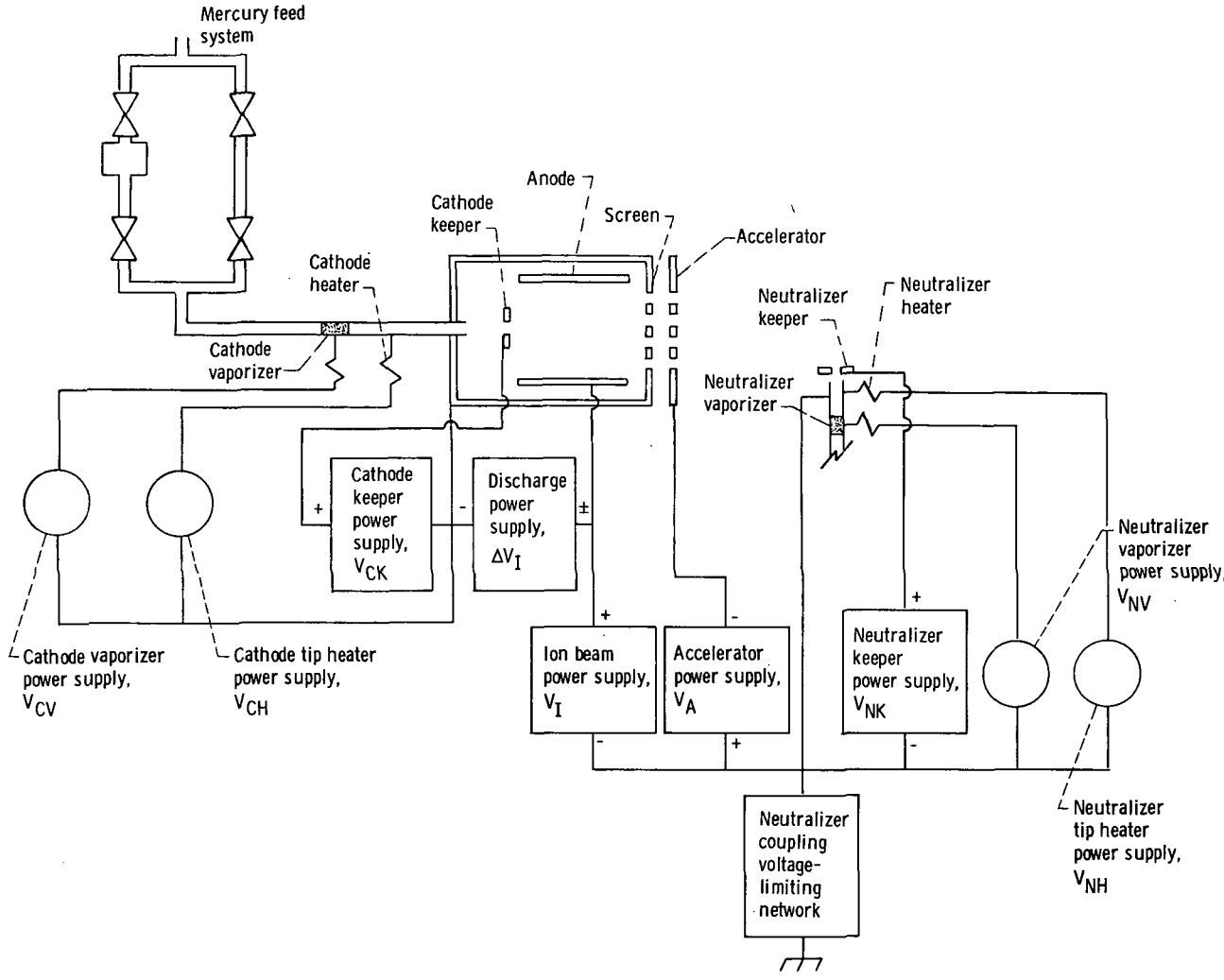

Figure 1. - Electrical diagram of interconnection of power supplies and 8-centimeter thruster.

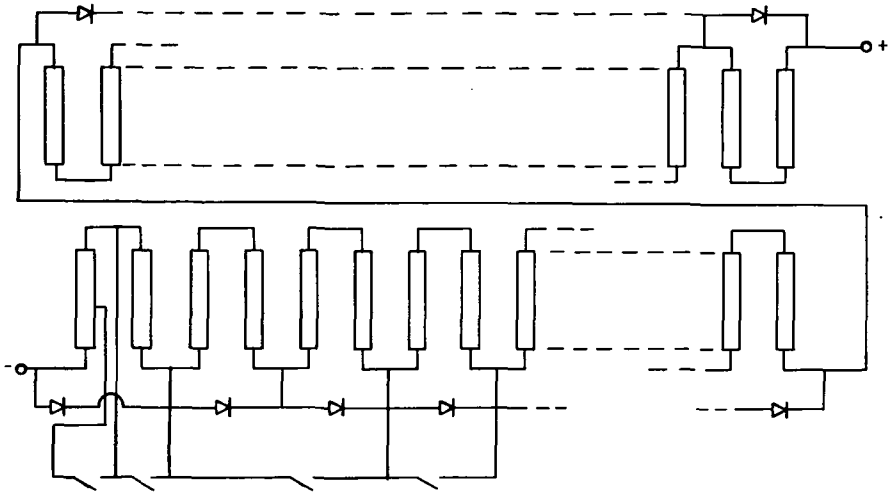

(a) Eighty series-connected 32-cell groups of 2 by 2 centimeter n on p silicon solar cells with bypass diodes and with cell-group shorting switches for load voltage regulation.

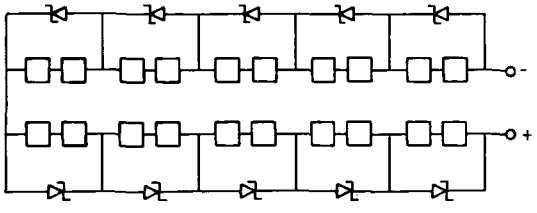

(b) Twenty series-connected 96-junction edge-illuminated solar cells with shunt-connected Zener diodes for load voltage regulation.

Figure 2. - Schematic diagrams of laboratory solar cell arrays.

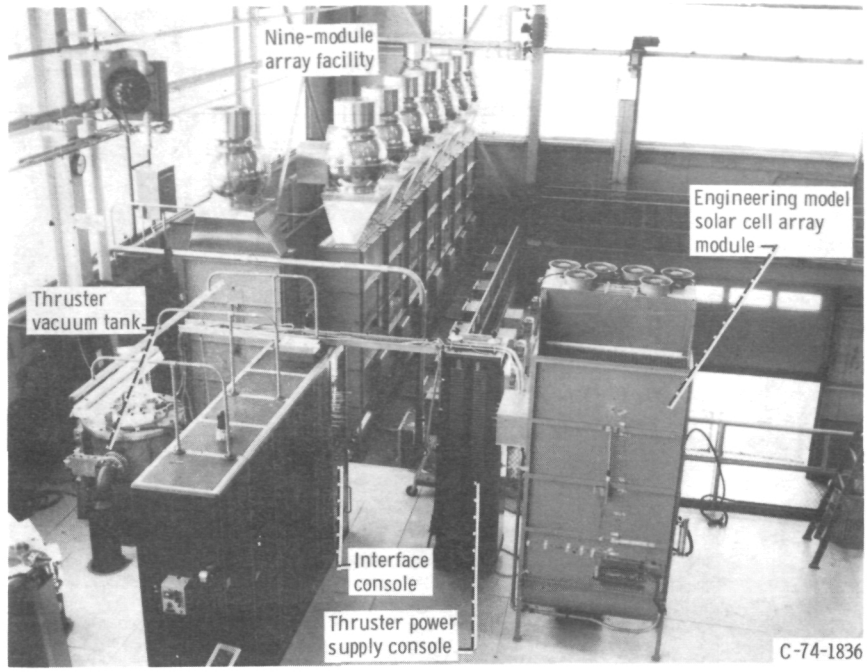

Figure 3. - Test equipment for solar array - thruster system test.

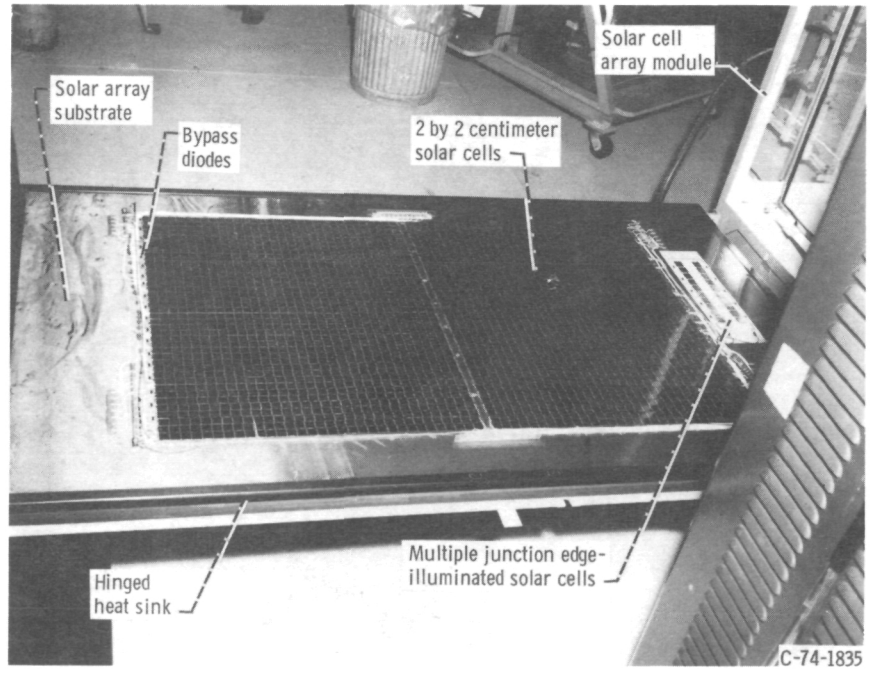

Figure 4. - Laboratory solar cell array mounted in support module heat sink.

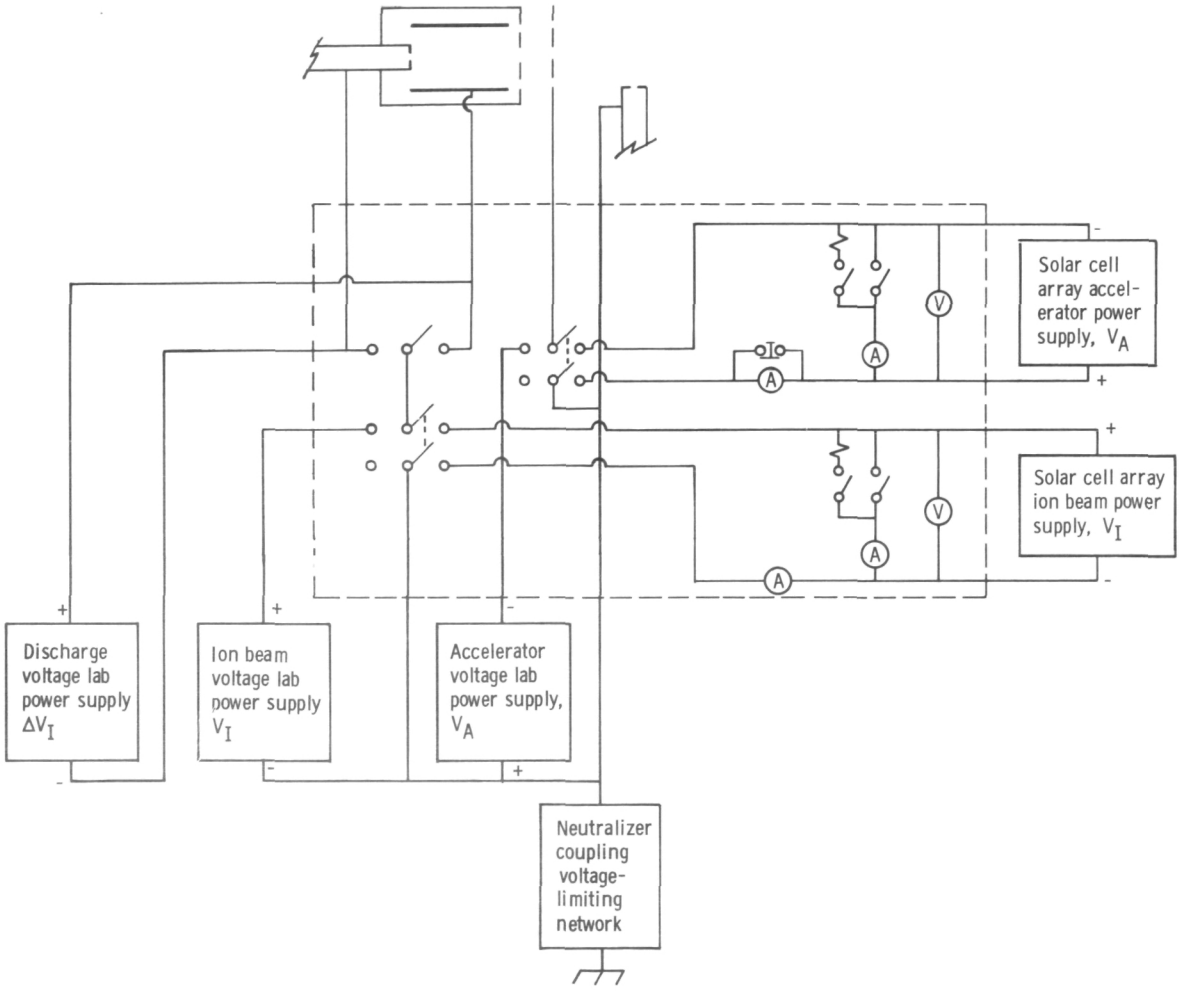

Figure 5. - Electrical interconnections of solar cell arrays, laboratory power supplies, thruster, and interface circuits.

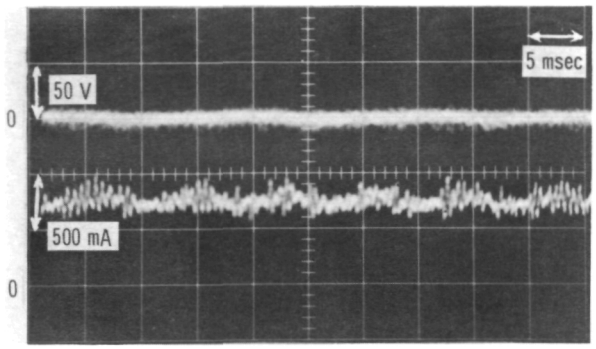

(a) Lower trace: discharge current (dc).

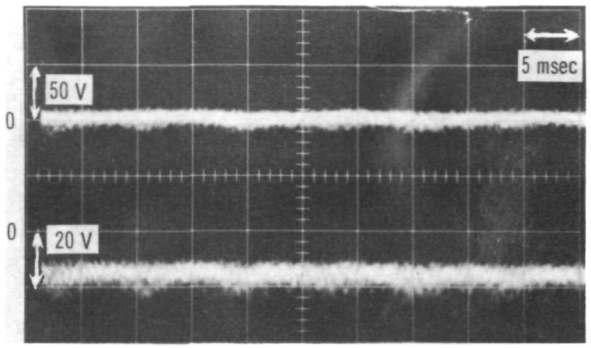

(b) Lower trace: neutralizer coupling voltage (dc).

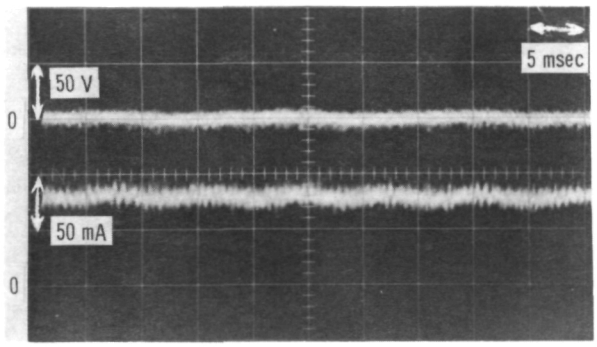

(c) Lower trace: beam current (dc).

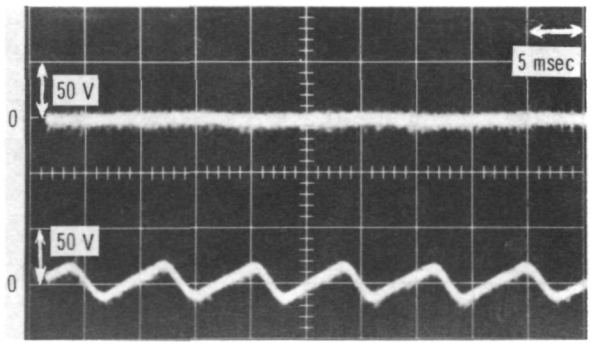

(d) Lower trace: sum of ac components of accelerator voltage and neutralizer coupling voltage.

Figure 6. - Selected waveforms with thruster beam and accelerator powered from conventional laboratory power supplies. Upper trace in all four parts: sum of ac components of beam voltage and neutralizer coupling voltage.

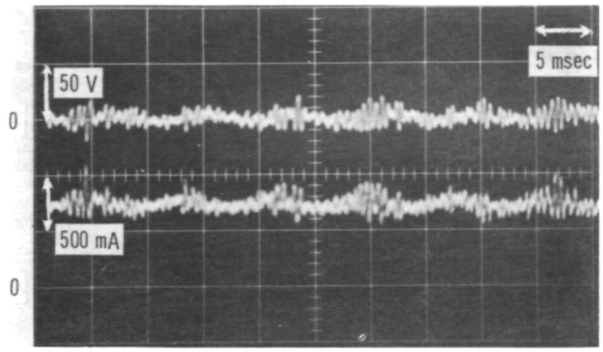

(a) Lower trace: discharge current (dc).

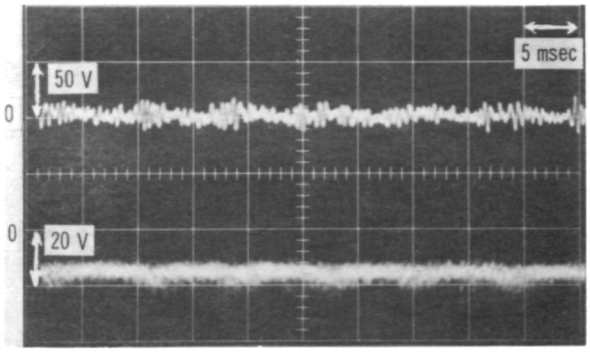

(b) Lower trace: neutralizer coupling voltage (dc).

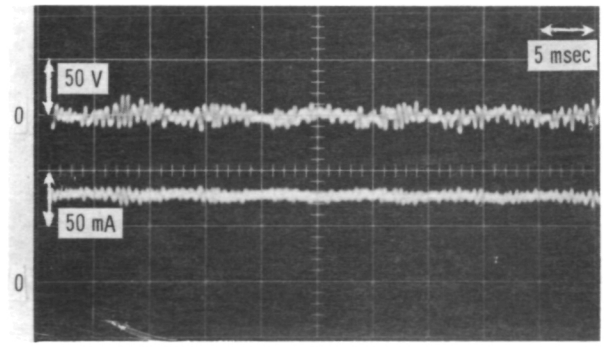

(c) Lower trace: beam current (dc).

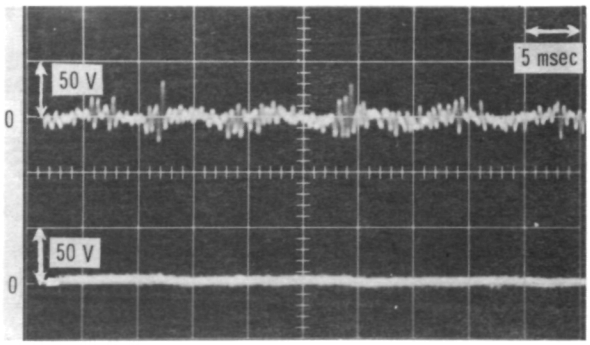

(d) Lower trace: sum of ac components of accelerator voltage and neutralizer coupling voltage.

Figure 7. - Selected waveforms with thruster beam and accelerator powered from laboratory solar cell arrays. Beam array short-circuit current, 1.67 times thruster beam current. Upper trace in all four parts: sum of ac components of beam voltage and neutralizer coupling voltage.

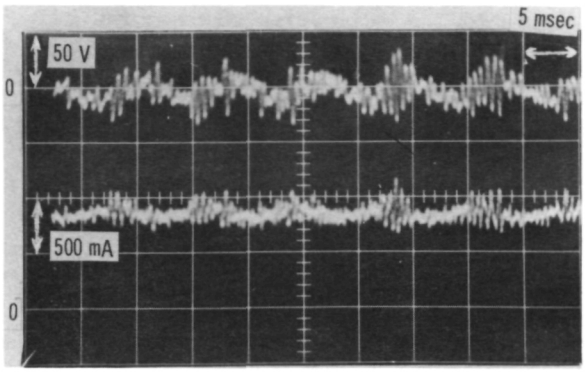

(a) Lower trace: discharge current (dc).

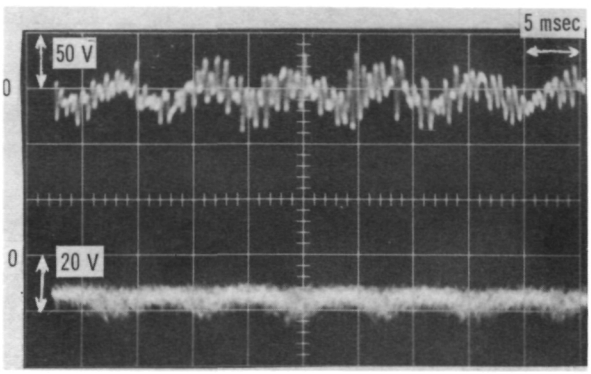

(b) Lower trace: neutralizer coupling voltage (dc).

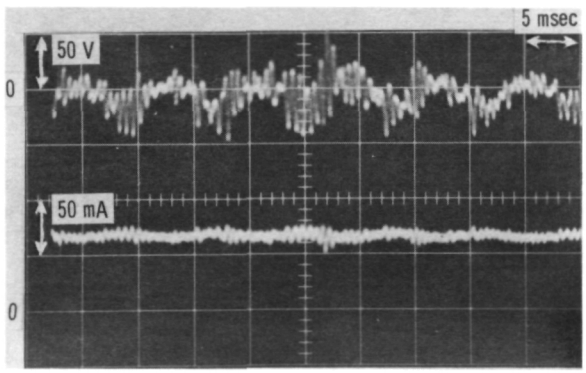

(c) Lower trace: beam current (dc).

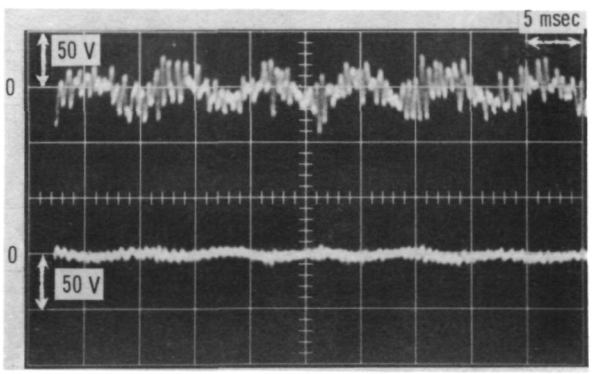

(d) Lower trace: sum of ac components of accelerator voltage and neutralizer coupling voltage.

Figure 8. - Selected waveforms with thruster beam and accelerator powered from laboratory solar cell arrays. Beam array short-circuit current, 1.25 times thruster beam current. Upper trace in all four parts: sum of ac components of beam voltage and neutralizer coupling voltage.

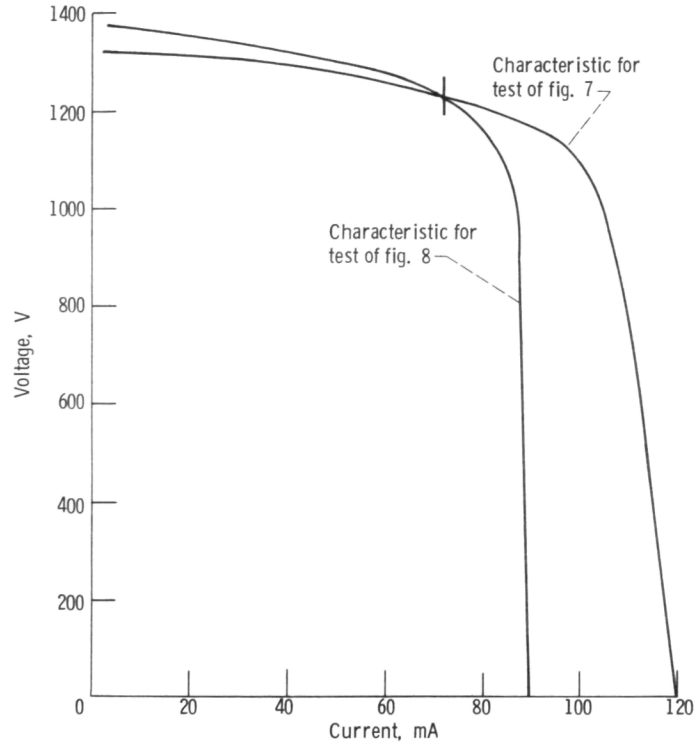

Figure 9. - Beam solar cell array voltage-current characteristics for standard and reduced illumination.

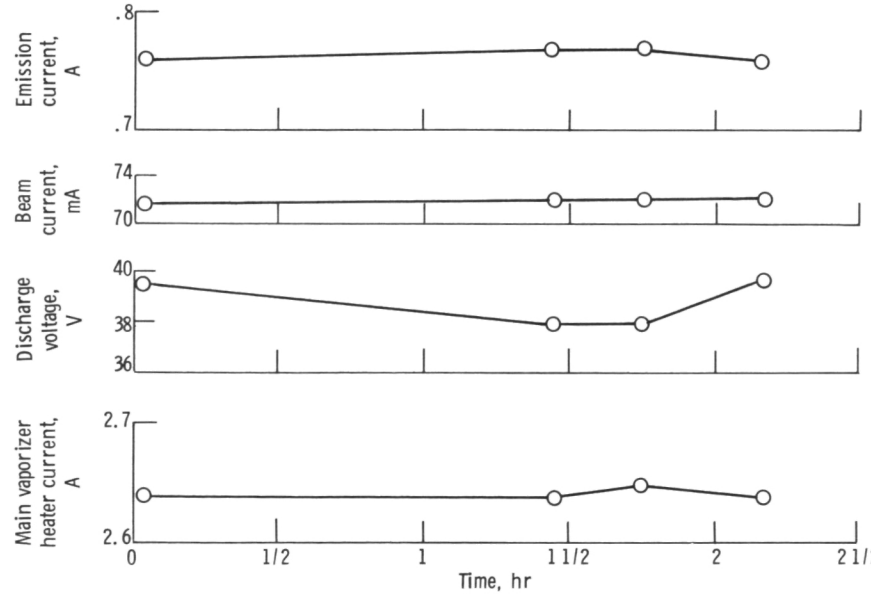

Figure 10. - Variation of selected thruster parameters during period of recording steady-state waveforms (manual thruster control).

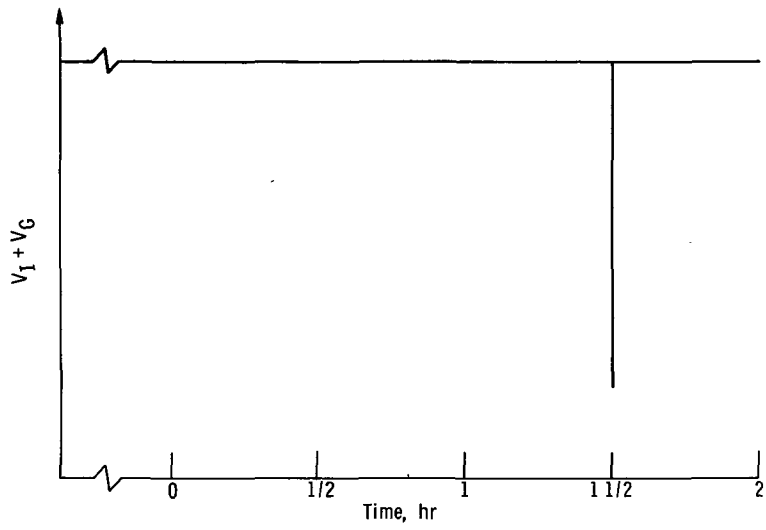

(a) Spark, at left, and short circuit followed by spontaneous recovery.

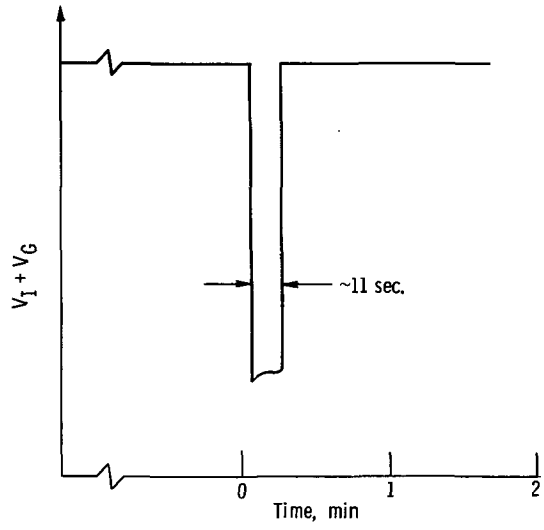

(b) Detail of spontaneous recovery portion.

Figure 11. - Typical recording of thruster beam voltage plus neutralizer coupling voltage ($V_I + V_G$) against time.

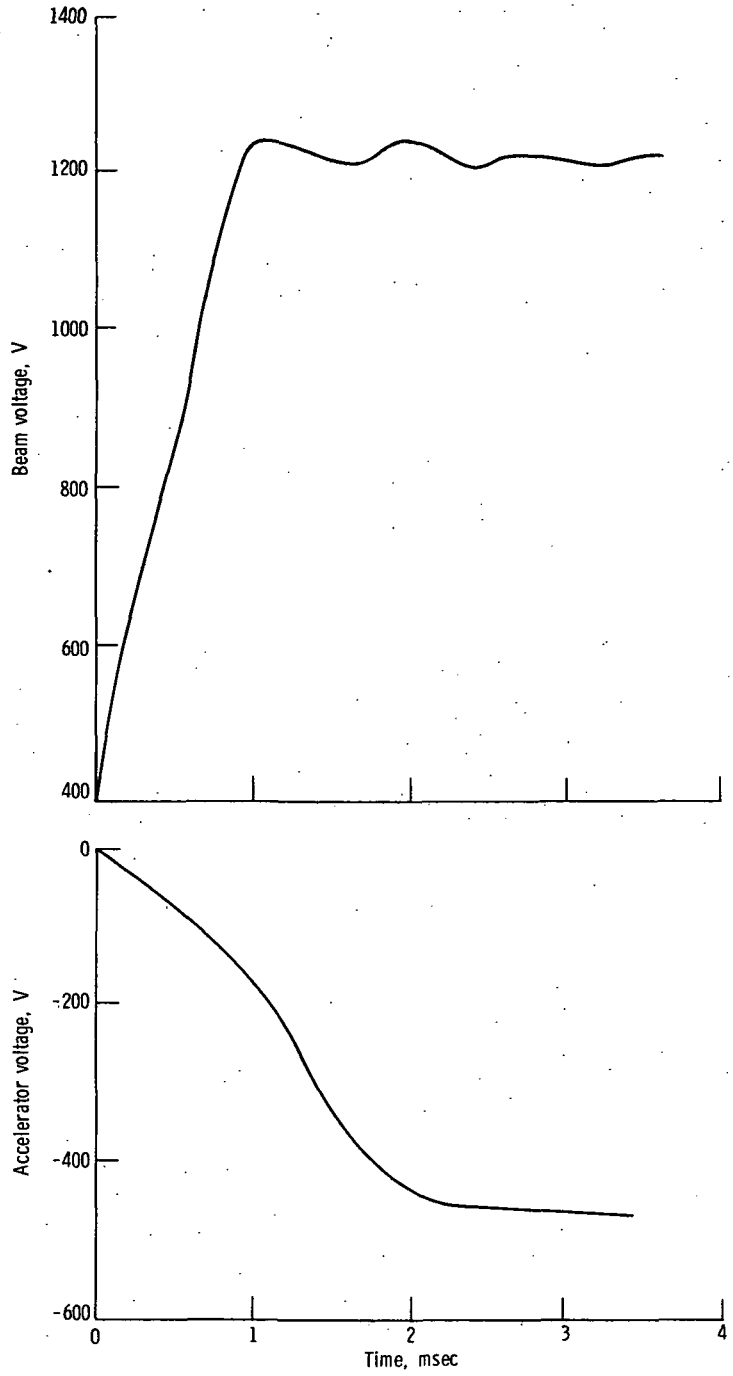

Figure 12. - Beam and accelerator solar array voltage excursions during spontaneous recovery from thruster beam short circuit.

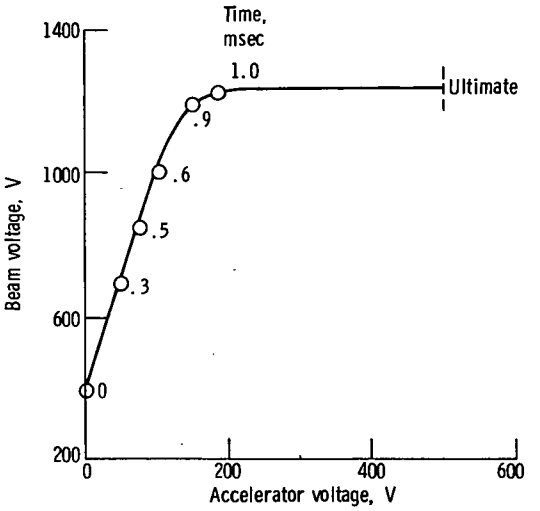

(a) Thruster beam and accelerator voltages (from fig. 12).

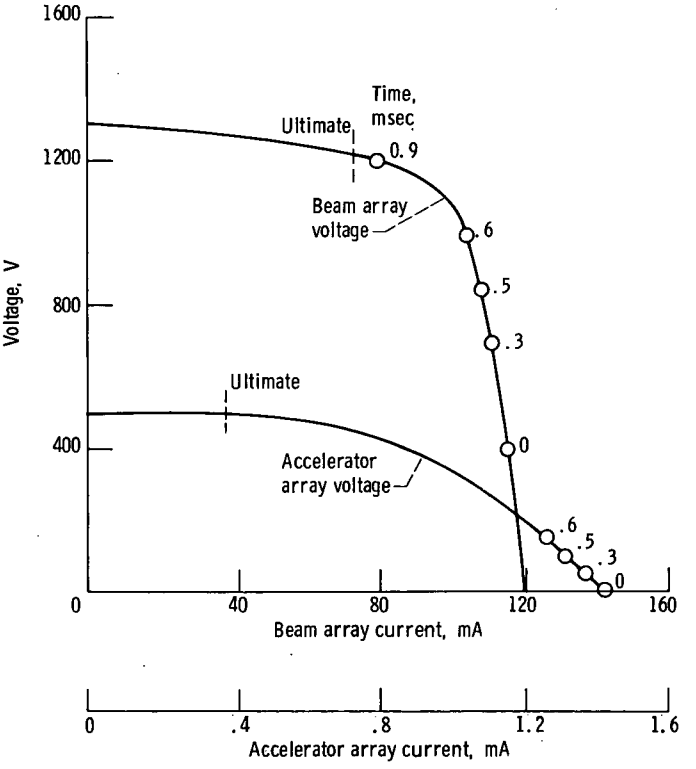

(b) Solar array characteristic curves showing simultaneous times during spontaneous recovery.

Figure 13. - Corresponding voltages and currents of beam and accelerator solar arrays during spontaneous recovery from thruster beam short circuit.

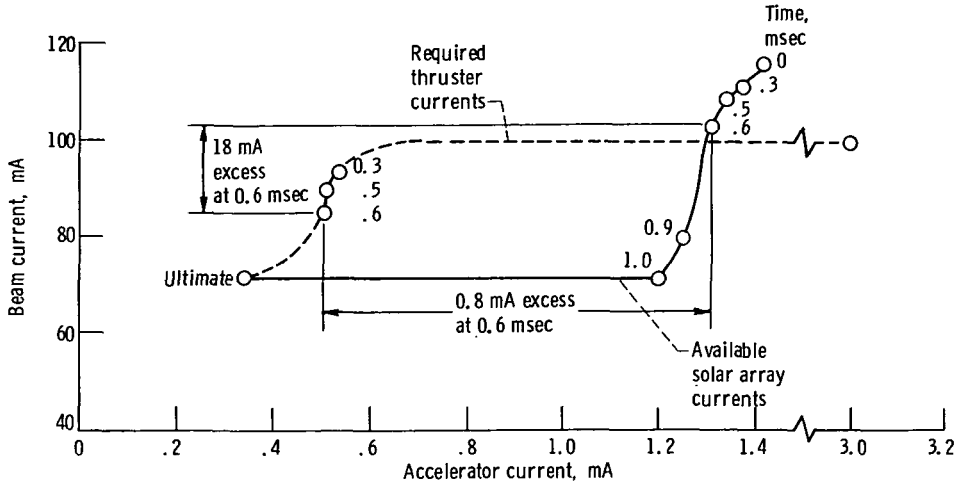

Figure 14. - Loci of available and required beam and accelerator currents during spontaneous recovery from beam short circuit.

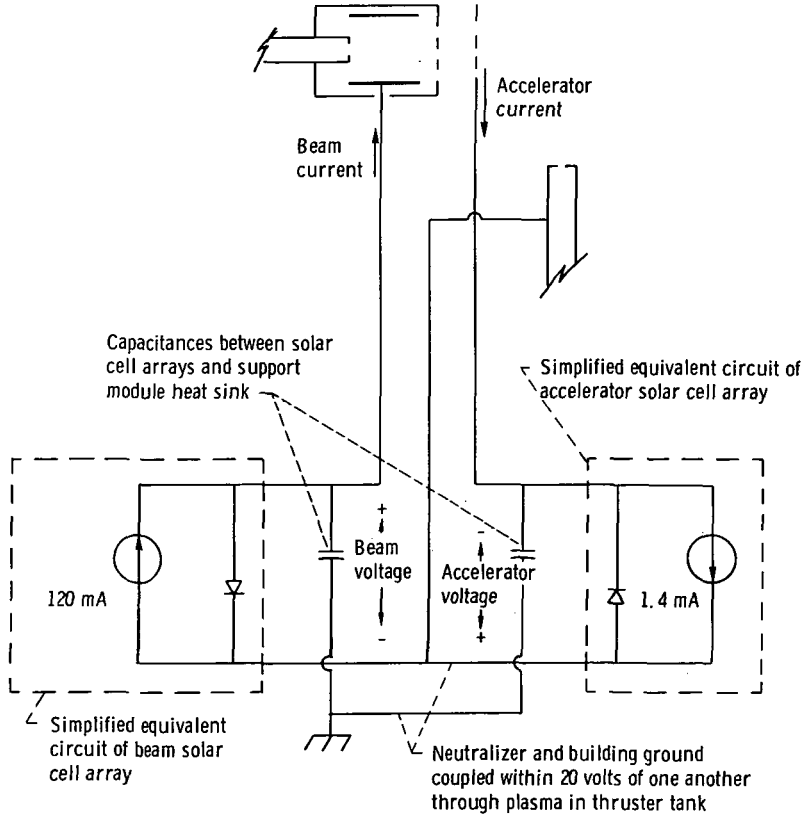

Figure 15. - Approximate equivalent circuit of thruster beam and accelerator solar cell arrays.

"The aeronautical and space activities of the United States shall be conducted so as to contribute . . . to the expansion of human knowledge of phenomena in the atmosphere and space. The Administration shall provide for the widest practicable and appropriate dissemination of information concerning its activities and the results thereof."

—NATIONAL AERONAUTICS AND SPACE ACT OF 1958

NASA SCIENTIFIC AND TECHNICAL PUBLICATIONS

TECHNICAL REPORTS: Scientific and technical information considered important, complete, and a lasting contribution to existing knowledge.

TECHNICAL NOTES: Information less broad in scope but nevertheless of importance as a contribution to existing knowledge.

TECHNICAL MEMORANDUMS: Information receiving limited distribution because of preliminary data, security classification, or other reasons. Also includes conference proceedings with either limited or unlimited distribution.

CONTRACTOR REPORTS: Scientific and technical information generated under a NASA contract or grant and considered an important contribution to existing knowledge.

TECHNICAL TRANSLATIONS: Information published in a foreign language considered to merit NASA distribution in English.

SPECIAL PUBLICATIONS: Information derived from or of value to NASA activities. Publications include final reports of major projects, monographs, data compilations, handbooks, sourcebooks, and special bibliographies.

TECHNOLOGY UTILIZATION PUBLICATIONS: Information on technology used by NASA that may be of particular interest in commercial and other non-aerospace applications. Publications include Tech Briefs, Technology Utilization Reports and Technology Surveys.

Details on the availability of these publications may be obtained from:

SCIENTIFIC AND TECHNICAL INFORMATION OFFICE

NATIONAL AERONAUTICS AND SPACE ADMINISTRATION

Washington, D.C. 20546